Smooth and nonsmooth dependence of Lyapunov vectors upon the angle variable on a torus in the context of torus-doubling transitions in the quasiperiodically forced Hénon map

Alexey Yu. Jalnine[1,*] and Andrew H. Osbaldestin[2]
[1]*Institute of Radio-Engineering and Electronics of RAS, Saratov Division, Zelenaya 38, Saratov 410019, Russia*
[2]*Department of Mathematics, University of Portsmouth, Portsmouth, PO1 3HE, United Kingdom*
(Received 10 July 2004; revised manuscript received 27 September 2004; published 10 January 2005)

A transition from a smooth torus to a chaotic attractor in quasiperiodically forced dissipative systems may occur after a finite number of torus-doubling bifurcations. In this paper we investigate the underlying bifurcational mechanism, which is responsible for the termination of the torus-doubling cascades on the routes to chaos in invertible maps under external quasiperiodic forcing. We consider the structure in the vicinity of a smooth attracting invariant curve (torus) in the quasiperiodically forced Hénon map and characterize it in terms of Lyapunov vectors, which determine the directions of contraction for an element of phase space in a vicinity of the torus. When the dependence of the Lyapunov vectors upon the angle variable on the torus is smooth, regular torus-doubling bifurcation takes place. On the other hand, we observe a transition consisting of the appearance of a nonsmooth dependence of the Lyapunov vectors upon the angle variable on the torus. We show that torus doubling becomes impossible after this transition has occurred, although the attractor of the system still remains a smooth torus. We illustrate how the transition terminates the torus-doubling bifurcation line in the parameter space with the torus transforming directly into a strange nonchaotic attractor. We argue that the transition plays a key role in mechanisms of the onset of chaos in quasiperiodically forced invertible dynamical systems.

DOI: 10.1103/PhysRevE.71.016206 PACS number(s): 05.45.−a

I. INTRODUCTION

The investigation of transition mechanisms from quasiperiodic dynamics to chaos is one of the central topics in contemporary nonlinear science. Starting with the classic works of Landau [1] and Ruelle and Takens [2], many researchers have undertaken theoretical [3–9] and experimental [10–13] studies of this problem. As is well known, the image of regular quasiperiodic motion in the phase space of a dissipative dynamical system is a smooth attracting ergodic torus. One convenient way to investigate mechanisms for the destruction of an ergodic torus is to consider quasiperiodically forced systems: in such systems the frequency ratios appear as independent parameters and can be effectively controlled in both numerics and in experiments. Quasiperiodically forced systems have become popular models for studies of the transition from quasiperiodicity to chaos after the discovery of a strange nonchaotic attractor (SNA) by Grebogi *et al.* in 1984 [14]. An SNA typically appears in the intermediate region between order and chaos and possesses a mixture of features of regular and chaotic attractors. Attractors of this type are nonchaotic in the sense that only nonpositive Lyapunov exponents occur, but they possess a fractal-like geometrical structure, which justifies the term "strange." (For more details on the structure and properties of SNA, see Refs. [15–22].)

One of the important observations, made in the 1980s by Anishchenko *et al.* [8] and Kaneko [9], is that the destruction of a smooth torus and the appearance of chaos may be preceded by a finite number of torus-doubling bifurcations. Therefore, much attention is focused on numerical [23–33] and experimental [34,35] studies of dynamical transitions in period-doubling systems under the effect of an external quasiperiodic force. When the amplitude of the external quasiperiodic force is fixed and the nonlinearity parameters of the model system are varied, a sequence of torus-doubling bifurcations can occur. Such a sequence is typically terminated by the onset of an SNA, followed by a further transition to chaos. The number of torus-doubling bifurcations in the sequence depends upon the amplitude of the external quasiperiodic force. For the case of sufficiently large amplitudes, a simple smooth torus may transform into an SNA. For small amplitude values, several torus-doubling bifurcations may occur before the SNA arises. The number of torus-doubling bifurcations grows as the amplitude of the quasiperiodic force is decreased. However, this number appears to be finite for any fixed nonzero amplitude. (See numerical results presented in Ref. [24].) An infinite bifurcation sequence can occur only for the case of the driving force amplitude equal to zero, as follows from the analysis developed in Ref. [23]. Thus an important issue is to understand the reason for the termination the torus-doubling cascades in the quasiperiodically forced systems.

For noninvertible unimodal maps the mechanism of the termination of torus-doubling cascades appears to be closely associated with the critical behavior studied by Kuznetsov *et al.* [26]. The line of torus-doubling bifurcation in the parameter space of the quasiperiodically forced logistic map terminates at a special critical point, called the torus-doubling terminal (TDT). (The corresponding values of the quasiperiodic force amplitude and the nonlinearity parameter will hereafter be referred to as the critical parameter values.) The termination of the bifurcation line is associated with the tangency of

*Electronic address: chaos777@rol.ru

the attractor with the line of zero derivative of the map. This event changes the character of the bifurcation, which becomes phase dependent and the attractor of the system becomes nonsmooth. For amplitudes of the quasiperiodic force above the critical value the sign of the derivative depends upon the angle variable on the torus; therefore, regular torus-doubling bifurcation becomes impossible. Numerical analysis shows that for small amplitudes of the quasiperiodic force a similar mechanism terminates the lines of doubling bifurcations for doubled, quadrupled, and other tori of this system [36]. Thus we can conclude that noninvertibility plays the role of a "terminator" for the torus-doubling cascades on the route to chaos in the quasiperiodically forced logistic map as well as for other noninvertible 1D maps of the same universality class.

It appears that the structure of the parameter space described above occurs in different period-doubling systems under external quasiperiodic forcing. For example, analogous transitions were observed in numerical experiments on a nonlinear dissipative oscillator under external two-frequency driving with irrational frequency ratio [37]. The Poincaré map in the phase space of such an oscillator is a smooth invertible three-dimensional (3D) map with one quasiperiodic variable. The most widely known example of such a kind is a quasiperiodically forced Hénon map [30,31]. A smooth closed invariant curve (torus) in the phase space of this map corresponds to the Poincaré section of the torus in the phase space of a biharmonically forced oscillator. Note that a reduction of the invertible 2D Hénon map in the limit of strong dissipation produces a noninvertible 1D logistic map. On the other hand, for dynamical systems determined by differential equations or for invertible maps, the mechanism of termination of the torus-doubling cascades obviously must be different from the above-mentioned loss of invertibility, which works only for noninvertible forced 1D maps.

In order to understand the underlying mechanism of the termination of the torus-doubling cascades in invertible systems, we consider in this paper the Hénon map driven by an external quasiperiodic force with an irrational frequency parameter, chosen to be the inverse golden mean. Since the torus-doubling bifurcation is local, we focus our attention on a study of the vicinity of a smooth attracting invariant curve (torus) in this system. Such a vicinity can be characterized in terms of Lyapunov vectors, which determine the directions of contraction for an element of phase volume around the attracting torus. The values of the Lyapunov vectors depend upon the angle variable on the torus. If the dependence of the Lyapunov vectors upon the angle variable is smooth, a torus-doubling bifurcation is possible. Alternatively, we observe a new transition, associated with the onset of a nonsmooth dependence of the Lyapunov vectors upon the angle variable on the torus. It is important to note that in a typical case the attractor of the system remains a smooth torus after such a transition. We show that the latter transition makes a regular torus-doubling bifurcation impossible and terminates the line of this bifurcation in the parameter space. We also argue that other regular (phase-independent) torus bifurcations such as symmetry breaking or inverse saddle-node bifurcation become impossible after the new transition has occurred. Therefore, further evolution of the attracting torus under variation of the parameters of the system is associated with the appearance of an SNA via phase-dependent mechanisms (such as torus fractalization [25,30], intermittency [32,33], or the Heagy and Hammel scenario [24,30]) or of a chaotic transient. We argue that an analogous mechanism may be responsible for the prevention of doubling bifurcations for doubled, quadrupled, and other tori of the model system.

The paper is organized as follows. In Sec. II we define Lyapunov vectors for quasiperiodic trajectories on a torus and use them for a description of the mechanism of torus-doubling bifurcation. In Sec. III we present numerical data and discuss smooth and nonsmooth dependences of Lyapunov vectors upon the angle variable for different parameter values of the model system. In Sec. IV we analyze dynamical transitions, which include doubling of tori, in the parameter space of the model system. In Sec. V we explain the mechanism which prevents the torus-doubling bifurcation from the viewpoint of the method of rational approximation [15]. In the Conclusion we discuss the role of the new phenomenon associated with the appearance of nonsmooth dependences of the Lyapunov vectors upon the angle variable on the torus in a general picture of transitions from quasiperiodicity to chaos, which involve different bifurcations of tori.

II. CHARACTERIZATION OF THE TORUS VICINITY: LYAPUNOV VECTORS AND INVARIANT 2D MANIFOLDS

Let us start with an autonomous Hénon map

$$x_{n+1} = a - x_n^2 + y_n,$$

$$y_{n+1} = bx_n, \tag{1}$$

where $0<b<1$. Let (x_0,y_0) be a fixed point of this map. The multipliers of the fixed point are defined as $\mu_{1,2} = (S \pm \sqrt{S^2-4J})/2$, where $J=-b$ is the determinant of the Jacobi matrix of the map (1) and $S=-2x_0$ is the trace of this matrix at the fixed point (x_0,y_0). Due to our choice of b, the condition $S^2-4J>0$ holds. The last condition implies that the fixed point possesses two different real multipliers $\mu_{1,2}(\mu_1\mu_2=-b)$, and, hence, the point is either a saddle or a stable node. For definiteness, let us suppose that $|\mu_1|>|\mu_2|$.

In the case of the saddle point ($|\mu_1|>1$, $|\mu_2|<1$), there are two invariant 1D manifolds (stable and unstable ones), which are represented by smooth invariant curves in the phase plane [see Fig. 1(a)]. The two eigenvectors $\mathbf{k}^{1,2}$ of the Jacobian matrix (Lyapunov vectors) give the directions tangent to the invariant manifolds at the fixed point.

When $|\mu_{1,2}|<1$, the fixed point is a stable node. In this case also we can define two Lyapunov vectors, which determine the directions of contraction for an element of phase space in a vicinity of the nodal fixed point. The *leading* vector $\mathbf{k}^1$, associated with the multiplier of largest modulus, is tangent to the set of stable invariant manifolds, as shown in Fig. 1(b). (See also Ref. [38].) The vector $\mathbf{k}^2$, referred to as the *nonleading* eigenvector, is tangent to the single "nonleading" stable invariant manifold.

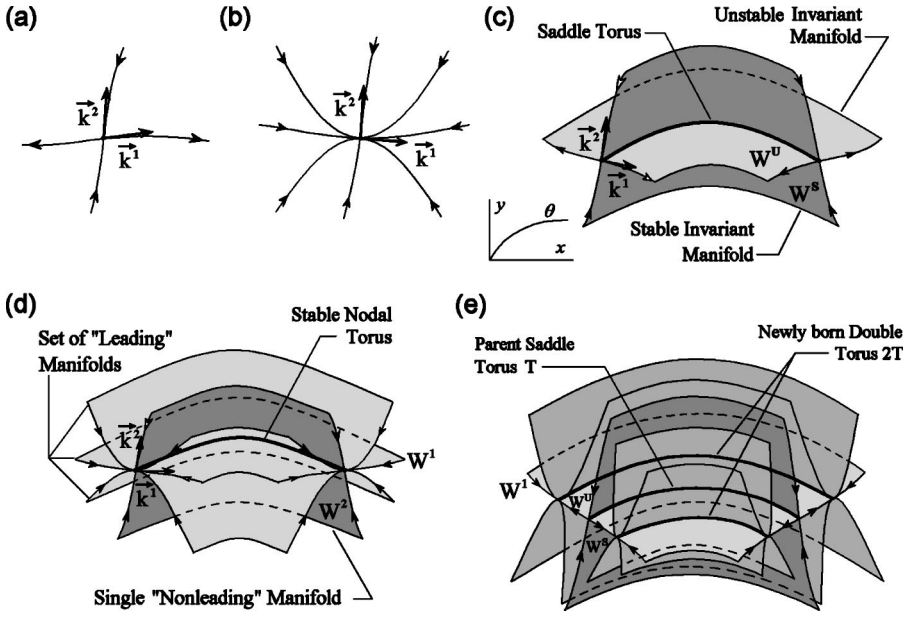

FIG. 1. Schematic drawings of the fixed points, tori, and associated invariant manifolds. (a) Saddle fixed point of the map (1). (b) Nodal fixed point of the map (1). (c) Saddle torus of the map (2). (d) Nodal torus of the map (2). (e) Parent saddle torus T and the newly-born double torus $2T$. The detailed explanations are provided in Sec. II of the paper.

Now we modify the map (1) by adding an external quasiperiodic force and consider the model map in $\mathbf{R}^2\times\mathbf{T}^1$:

$$x_{n+1} = a - x_n^2 + y_n + \varepsilon \cos 2\pi\theta_n,$$

$$y_{n+1} = bx_n,$$

$$\theta_{n+1} = \theta_n + \omega \ (\mathrm{mod}\ 1), \tag{2}$$

where ω is an irrational number, which we set equal to the inverse golden mean: $\omega=(\sqrt{5}-1)/2$. For $\varepsilon=0$ map (2) has a trivial invariant curve (torus)

$$T_0:\{(x,y,\theta) \in \mathbf{R}^2 \times \mathbf{T}^1 | x = x_0, y = y_0, \theta \in [0,1)\}.$$

Obviously, in this case a structure of a vicinity of the torus T_0 will be determined by multipliers of the fixed point (x_0,y_0).

If $|\mu_1|>1$ and $|\mu_2|<1$, the torus T_0 is of a saddle type, and there are two invariant manifolds, unstable and stable, which we denote as W^u and W^s, respectively. The manifolds are represented by smooth 2D surfaces in the 3D phase space, as shown in Fig. 1(c). At any point of the saddle torus one can define two directions, which are tangent to the invariant manifolds and orthogonal to the axis of the angle variable θ. For $\varepsilon=0$ these directions are given simply by the Lyapunov vectors $\mathbf{k}^{1,2}$ of the fixed point (x_0,y_0) of the map (1).

Likewise, if $|\mu_{1,2}|<1$, the torus T_0 is of a stable nodal type, and, again, at any point of a stable nodal torus one can define two Lyapunov vectors, which determine two directions of contraction for an element of phase space in vicinity of the torus. The rate of contraction in each direction is characterized by the respective Lyapunov exponent ($\sigma_{1,2}=\ln|\mu_{1,2}|$). If we introduce 2D stable invariant manifolds associated with the nodal torus [as extensions of the 1D invariant manifolds of the nodal fixed point of the map (1)], then the two Lyapunov vectors $\mathbf{k}^{1,2}$ will define two directions tangent to the manifolds and orthogonal to the axis of angle variable θ [see Fig. 1(d)]. The leading vector $\mathbf{k}^1$ is tangent to a continuum of stable 2D manifolds (we arbitrarily choose one of them and refer it to as W^1), while the vector $\mathbf{k}^2$ is tangent to one special nonleading stable manifold W^2. The remainder of this article is concerned with the stable nodal torus and its vicinity.[1]

Now let $\varepsilon\neq 0$. For typical values of a and b apart from the bifurcation points of the map (2), a small quasiperiodic perturbation will not destroy the torus and the smooth 2D manifolds. Thus, for small nonzero ε the map (2) possesses a nontrivial torus

$$T:\{(x,y,\theta) \in \mathbf{R}^2 \times \mathbf{T}^1 | x = x(\theta), y = y(\theta), \theta \in [0,1)\}; \tag{3}$$

the stable 2D manifolds $W^{1,2}$ in a vicinity of the torus T become distorted, but remain smooth 2D surfaces. The Lyapunov vectors, which are tangent to the manifolds and orthogonal to the θ axis, now depend on the angle variable θ: $\mathbf{k}^{1,2}=\mathbf{k}^{1,2}(\theta)$. While the manifolds are smooth, the vector functions $\mathbf{k}^{1,2}(\theta)=(k_x^{1,2}(\theta),k_y^{1,2}(\theta),0)$ remain differentiable. As the parameter ε increases [other parameters of the map (2) we suppose to be fixed], the plots of the functions $k_{x,y}^{1,2}(\theta)$ may become more and more distorted, until these functions lose differentiability at some critical value of ε. The appearance of nonsmooth dependences of the Lyapunov vectors

[1]Note that, besides stable nodes and saddles, a dissipative map may possess a fixed point of focal type, which is characterized by complex conjugate multipliers ($\mu_1=\mu_2^*$). In this case the addition of the quasiperiodic variable θ gives a smooth torus that has a vicinity of focal type. The Lyapunov vectors are not defined in the focus. Therefore, the 2D invariant manifolds turn around the stable torus of focal type. In fact, the one time iterated Hénon map (1) does not possess focal fixed points at $b>0$. However, it has stable periodic orbits of periods 2^n, $n\geqslant 2$, which are characterized by complex values of $\mu_{1,2}$. Further we will observe some quasiperiodic regimes arising from focal periodic orbits, although they do not play a significant role in the present work.

$\mathbf{k}^{1,2}$ upon the angle variable θ apparently provides evidence for the destruction of the smooth 2D manifolds in a vicinity of the torus T.

Let us discuss the role of Lyapunov vectors and 2D invariant manifolds in the mechanism of the torus-doubling bifurcation in the map (2). On the threshold of bifurcation, the map possesses a nodal torus T, shown in Fig. 1(d). As a control parameter of the system passes through the bifurcation value, the nodal torus T loses stability and becomes of a saddle type. The loss of stability of the torus T occurs along the less stable leading direction $\mathbf{k}^1(\theta)$, as the corresponding Lyapunov exponent σ_1 passes through zero. A pair of smooth curves $2T$ ("double torus") appears in a vicinity of $2T$; a trajectory on the double torus visits two curves alternately. The leading manifold W^1 of the parent nodal torus T transforms after bifurcation into the unstable manifold W^u of the saddle torus T. The newly born double torus $2T$ belongs to the smooth manifold W^u, as shown in Fig. 1(e). Note that the vector function $\mathbf{k}^1(\theta)$ determines the direction tangent to W^u. Hence, immediately after the bifurcation the vector function $\mathbf{k}^1(\theta)$ determines in linear approximation the direction from the saddle torus T to the newly born double torus $2T$. Since all the tori (T and $2T$) are smooth and they belong to the smooth manifold W^u, the dependence $\mathbf{k}^1(\theta)$ will be also smooth. On the other hand, the nonsmooth dependence of $\mathbf{k}^1(\theta)$ upon θ would imply that a newly born object (born instead of $2T$) must also be nonsmooth as it belongs to a nonsmooth manifold W^u. Thus, existence a smooth vector function $\mathbf{k}^1(\theta)=(k_x^1(\theta),k_y^1(\theta),0)$ appears to be a necessary condition for a possibility of the regular torus-doubling bifurcation. The loss of smoothness of the dependence $\mathbf{k}^1(\theta)$ provides us with evidence that torus-doubling bifurcation becomes impossible. Let us consider now the methods for numerical computation of the dependences $\mathbf{k}^{1,2}(\theta)$ and for the analysis of their smoothness.

First, let us turn to a case when the functions $\mathbf{k}^{1,2}(\theta)$ are smooth. Let there be a point (x_0,y_0,θ_0), which belongs to the torus (3). In order to define the Lyapunov vectors $\mathbf{k}^{1,2}(\theta_0)$ at this point, we iterate map (2) starting from (x_0,y_0,θ_0) and obtain an orbit $(x_0,y_0,\theta_0),(x_1,y_1,\theta_1),\ldots,(x_n,y_n,\theta_n)$. Let a vector $\mathbf{k}_0$ be collinear to the vector $\mathbf{k}^1(\theta_0)$ [or $\mathbf{k}^2(\theta_0)$] at the initial point. After one iteration of map (2), this vector will be mapped into the vector $\mathbf{k}^1$, which is collinear to the vector $\mathbf{k}^1(\theta_1)$ [or $\mathbf{k}^2(\theta_1)$] at the point (x_1,y_1,θ_1). The evolution of $\mathbf{k}_0$ is described by the Jacobi matrix of the map (2):

$$\mathbf{k}_1=\hat{\mathbf{J}}(x_0,y_0,\theta_0)\mathbf{k}_0. \tag{4}$$

After n iterations the operator $\hat{\mathbf{J}}^{(n)}$ of evolution of the vector is

$$\hat{\mathbf{J}}^{(n)}=\hat{\mathbf{J}}(x_{n-1},y_{n-1},\theta_{n-1})\hat{\mathbf{J}}(x_{n-2},y_{n-2},\theta_{n-2})\cdots\hat{\mathbf{J}}(x_0,y_0,\theta_0).$$

Thus, we obtain a sequence of vectors $\mathbf{k}_1,\mathbf{k}_2,\ldots,\mathbf{k}_n$, with $\mathbf{k}_n=\hat{\mathbf{J}}^{(n)}\mathbf{k}_0$, which are collinear to the Lyapunov vectors at the respective points of the orbit. Now, in order to define the initial vector $\mathbf{k}_0$, we consider a subsequence of the trajectory points which converges to the initial point (x_0,y_0,θ_0). Since we have chosen ω equal to the inverse golden mean, we take the subsequence $(x_{F_0},y_{F_0},\theta_{F_0}),\ldots,(x_{F_k},y_{F_k},\theta_{F_k})$, where $F_k=1,2,3,5,8,13,\ldots$ are the Fibonacci numbers. Under the assumption of smoothness of $\mathbf{k}^{1,2}(\theta)$, the sequence of vectors $\mathbf{k}_{F_0},\ldots,\mathbf{k}_{F_k}$ also converges to the vector $\mathbf{k}_0$ at the initial point. Hence, we come to a conclusion that

$$\mathbf{k}_{F_k}=\hat{\mathbf{J}}^{(F_k)}\mathbf{k}_0\rightarrow\mu_{F_k}\mathbf{k}_0 \quad \text{as} \quad k\rightarrow\infty, \tag{5}$$

where μ_{F_k} is a coefficient. Thus, we obtain an eigenvalue problem for the matrix

$$\hat{\mathbf{J}}^{(F_k)}=\begin{bmatrix} J_{11} & J_{12} & J_{13} \\ J_{21} & J_{22} & J_{23} \\ 0 & 0 & 1 \end{bmatrix}.$$

One of the eigenvectors of the matrix $\hat{\mathbf{J}}^{(F_k)}$ corresponds to a trivial unit eigenvalue associated with the angle variable. The other two eigenvectors have the form $\mathbf{m}_{F_k}^{1,2}=(m_x^{1,2},m_y^{1,2},0)$, orthogonal to the axis of the angle variable. Hence, at the point (x_0,y_0,θ_0), one can define two Lyapunov vectors $\mathbf{k}^{1,2}(\theta_0)$ as the limits for eigenvectors $\mathbf{m}_{F_k}^{1,2}$ at $k\rightarrow\infty$. Analogous arguments can be developed for any point (x,y,θ) of the torus (3). Note that relation (5) makes it possible to determine two nontrivial Lyapunov exponents for a quasiperiodic trajectory on the torus as

$$\sigma_{1,2}=\lim_{k\rightarrow\infty}(1/F_k)\ln|\mu_{F_k}^{1,2}|.$$

In the limit $k\rightarrow\infty$ the values of $\sigma_{1,2}$ do not depend on the initial phase θ_0 and characterize the entire torus, since the quasiperiodic trajectory fills the torus densely due to ergodicity of the quasiperiodic motion.

In practice, the method of definition of the Lyapunov vectors described above is inconvenient for numerical computations. Moreover, the method was based on an assumption of differentiability of $\mathbf{k}^{1,2}(\theta)$. On the other hand, we should take into account that such dependences can be either differentiable or nondifferentiable. Nevertheless, due to the possibility of definition of $\mathbf{k}^{1,2}$ as the eigenvectors of an operator [see Eq. (5)], we can suggest another simple way for their determination.

Let us suppose that the vector functions $\mathbf{k}^{1,2}(\theta)$ corresponding to the leading and nonleading Lyapunov vectors are normalized to unity at any point of the torus (3). We can consider the evolution of an arbitrarily chosen vector $\mathbf{k}_0=(k_{x,0},k_{y,0},0)$ along the trajectory $(x_0,y_0,\theta_0),(x_1,y_1,\theta_1),\ldots,(x_n,y_n,\theta_n)$ under iterations of the linearized map (4). Multiplying by the Jacobian matrix at each point of the trajectory and then normalizing, we obtain the map

$$\begin{aligned} \mathbf{k}'_{n+1}&=\hat{\mathbf{J}}(x_n,y_n,\theta_n)\mathbf{k}_n, \\ \mathbf{k}_{n+1}&=|\mathbf{k}'_{n+1}|^{-1}\mathbf{k}'_{n+1}, \\ \theta_{n+1}&=\theta_n+\omega \pmod 1. \end{aligned} \tag{6}$$

As we know, in a typical case, after a sufficiently large number of iterations, an arbitrarily assigned vector tends to the

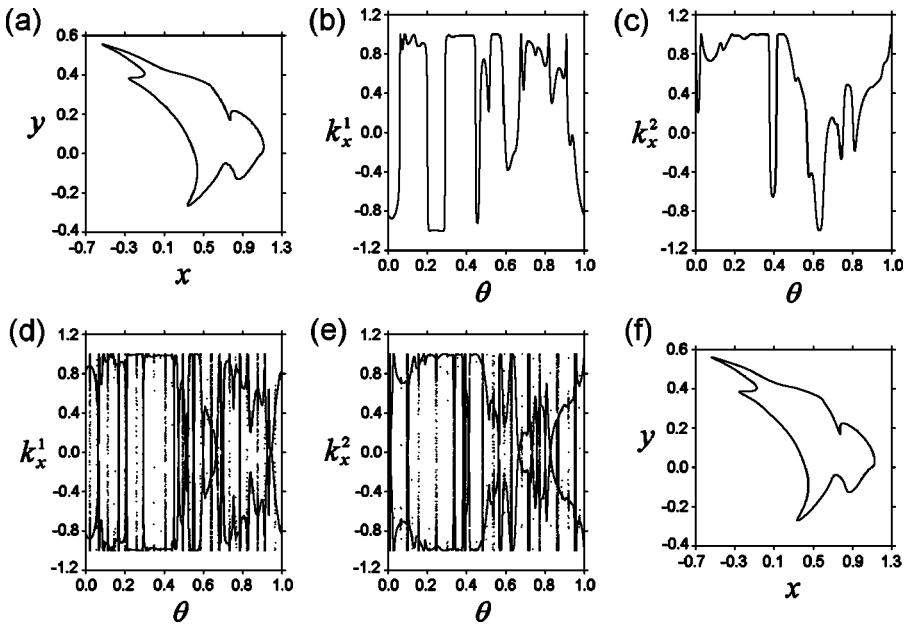

FIG. 2. (a) Attracting torus of the map (2) at $a=0.55$, $\varepsilon=0.6$. (b) Plot of the function $k_x^1(\theta)$ at $a=0.55$, $\varepsilon=0.6$ [only odd iterations of the map (6) are plotted]. (c) Plot of the function $k_x^2(\theta)$ at $a=0.55$, $\varepsilon=0.6$ [image of the torus of the map (7)]. (d) SNA of the map (6) at $a=0.559$, $\varepsilon=0.6$. (e) SNA of the map (7) at $a=0.559$, $\varepsilon=0.6$. (f) Attracting torus of the map (2) at $a=0.559$. We have chosen $b=0.5$ for these and all the following figures.

direction corresponding to the largest Lyapunov exponent (e.g., Ref. [39]). Since we have chosen $\mathbf{k}_0$ initially orthogonal to the phase axis, this direction will be given by the leading Lyapunov vector $\mathbf{k}^1(\theta)$. Thus, $\mathbf{k}_n$ tends to $\pm\mathbf{k}^1(\theta_n)$ as $n\to\infty$. A plot of the function $\pm\mathbf{k}^1(\theta)$ may be interpreted as an image of the attractor of the map (6). Note that for any quasiperiodic trajectory on the torus (3) the values x_n and y_n are functions of the angle variable θ_n: $x_n=x(\theta_n), y_n=y(\theta_n)$. This fact makes it possible to consider the map (6) as a usual quasiperiodically forced map and allows us to use standard methods for the analysis of its dynamical regimes. For instance, to obtain the leading Lyapunov vector $\mathbf{k}^1(\theta_0)$ at the point (x_0, y_0, θ_0) on the torus, we should start iterating Eqs. (6) from the initial angle $\theta_{-n}[=\theta_0-n\omega(\mathrm{mod}\ 1)]$, where n is sufficiently large, with an arbitrarily chosen initial condition $\mathbf{k}_{-n}$.

Now let us consider possible types of attractors of the map (6). In the context of further numerical analysis, the following three cases appear to be essential.

(C1) The map has two attractors represented by smooth invariant curves $\pm\mathbf{k}^1(\theta)$, which are symmetric with respect to the axis of angle variable θ.

(C2) The map has one attractor, which consists of two smooth curves $\pm\mathbf{k}^1(\theta)$, visited alternately at iterations of the map.

(C3) The attractor of the map is *strange nonchaotic*, represented by the nonsmooth[2] and double-valued function $\pm\mathbf{k}^1(\theta)$.

In cases (C1) and (C2) the function $\mathbf{k}^1(\theta)$ is differentiable. It implies a smooth character of the dependence of the leading Lyapunov vector upon the angle variable on the torus (3). The appearance of a strange nonchaotic attractor in the map (6) [case (C3)] provides evidence of a loss of differentiability of the vector function $\mathbf{k}^1(\theta)$. Hence, in the last case, the dependence of the leading Lyapunov vector upon the angle variable is nonsmooth.[3]

In the same way, we can determine the nonleading Lyapunov vector $\mathbf{k}^2(\theta)$, which corresponds to the second nontrivial Lyapunov exponent. For this, we invert the map (2) and consider an evolution of some arbitrary chosen vector $\mathbf{k}_0$ under iteration of the inverse map along the quasiperiodic trajectory on the torus (3). Taking into account a normalization of the vector, we represent the evolution map as

$$\mathbf{k}'_{n+1}=\hat{\mathbf{J}}^{-1}(x_n,y_n,\theta_n)\mathbf{k}_n,$$

$$\mathbf{k}_{n+1}=|\mathbf{k}'_{n+1}|^{-1}\mathbf{k}'_{n+1},$$

$$\theta_{n+1}=\theta_n-\omega\ (\mathrm{mod}\ 1). \tag{7}$$

Here $\hat{\mathbf{J}}^{-1}(x,y,\theta)$ is the Jacobian matrix of the map inverse to the quasiperiodically forced Hénon map (2). Since the maps (6) and (7) are inverse with respect to each other, they possess identical invariant sets. Note that the attracting invariant set of Eqs. (6) [defined as $\pm\mathbf{k}^1(\theta)$] is a repellor for the map (7), while the attractor of the map (7) [given by $\pm\mathbf{k}^2(\theta)$] appears to be the repelling invariant set of the map (6). Hence, under iterations of Eqs. (7) the vector $\mathbf{k}_n$ will tend to $\pm\mathbf{k}^2(\theta_n)$ as $n\to\infty$.

[2]According to the results of Stark (see Ref. [19]), an SNA cannot be the graph of a continuous function. Strictly speaking, the function $\pm\mathbf{k}^1(\theta)$ must be nonsmooth and upper-lower semicontinuous.

[3]In a general case we should consider one more possibility: (C4) the attractor of the map (6) represents a three-frequency torus. In this case the vector-function $\mathbf{k}^1(\theta)$ cannot be defined. This situation takes place when the quasiperiodic forcing is added to a system with a focal fixed point. As we has already mentioned, the Hénon map does not possess such points for $b>0$. However, the three-frequency quasiperiodic regime may be observed in the system (6) when we investigate the structure of the vicinity of a double torus $2T$ or quadruple torus $4T$ of the map (2).

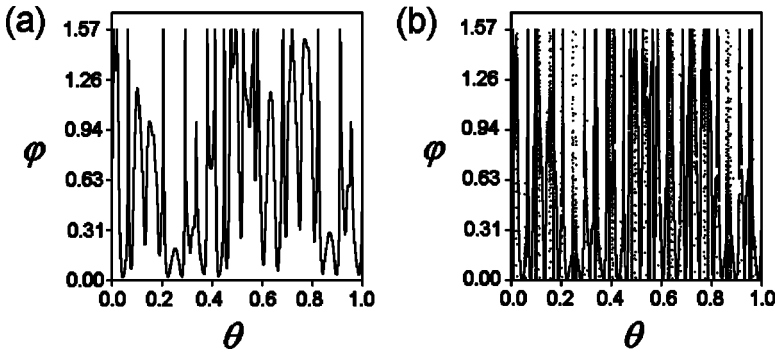

FIG. 3. Dependence of the angle φ between Lyapunov vectors upon the angle coordinate θ: (a) at $a=0.556$ (slightly below the critical value a_c), $\varepsilon=0.6$, (b) at $a=0.559$ (slightly above the critical value a_c), $\varepsilon=0.6$.

Thus, the problem of the analysis of the dependences of leading and nonleading Lyapunov vectors $\mathbf{k}^{1,2}$ upon the angle variable θ is reduced to the analysis of the attractors of the maps (6) and (7) in the space of Lyapunov vectors. Smoothness of the attractors represented by vector functions $\pm\mathbf{k}^{1,2}(\theta)$ implies smoothness of the dependences of Lyapunov vectors on the torus (3) upon the angle variable. The onset of strange nonchaotic attractors in the maps (6) and (7) indicates the loss of smoothness of the dependences of Lyapunov vectors $\pm\mathbf{k}^{1,2}$ upon the angle variable θ and, as a consequence, the destruction of smooth 2D invariant manifolds in a vicinity of the nodal torus (3).

III. LOSS OF DIFFERENTIABILITY OF THE DEPENDENCE OF LYAPUNOV VECTORS UPON THE ANGLE VARIABLE

Let us fix $b=0.5$ and $\varepsilon=0.6$, and consider the evolution of the attractor of the map (2) and the attractors of Eqs. (6) and (7) in the Lyapunov space under variation of the parameter a.

At $a=0.55$ the attractor of the map (2) is a smooth torus [Fig. 2(a)]. The attractor of the map (6) is a double torus; i.e., it is represented by a pair of smooth curves $\pm\mathbf{k}^1(\theta)$, which map onto each other under iteration. The resulting plot of the function $k_x^1(\theta)$ is presented in Fig. 2(b). The map (7) possesses two attracting invariant tori $\pm\mathbf{k}^2(\theta)$, which are symmetric with respect to the axis of angle variable θ. The plot of the function $k_x^2(\theta)$ is shown in Fig. 2(c). One can see that both functions $k_x^{1,2}(\theta)$ are smooth: the Lyapunov vectors depend smoothly upon the angle variable θ. As a is increased, the smooth vector functions $\pm\mathbf{k}^{1,2}(\theta)$ corresponding to attractors of the maps (6) and (7) become more and more distorted at small scales, until strange nonchaotic attractors arise simultaneously in Eqs. (6) and (7) at the critical value $a_c \simeq 0.559$. The plots of the functions $k_x^{1,2}(\theta)$ at $a=0.559$ are presented in Figs. 2(d) and 2(e). Thus, the dependences of the Lyapunov vectors upon the angle variable become nondifferentiable. Note that the attractor of the map (2) still remains a smooth torus, as shown in Fig. 2(f). The transition to SNA in this map (2) occurs only at $a_f \simeq 0.656$.

A smooth torus characterized by nonsmooth dependences $\mathbf{k}^{1,2}(\theta)$ can be observed for all values of the parameter a within the interval $a \in [a_c, a_f)$. Numerical analysis shows that besides this interval there are other intervals of a with nonsmooth dependences of the Lyapunov vectors upon the angle coordinate: $a \in [0.266, 0.416]$ and $a \in [0.484, 0.521]$. However, we emphasize that this is the first interval $[a_c, a_f)$, which is important for an explanation of the direct transition from smooth torus to SNA without torus-doubling bifurcation in the system (2). Nonsmooth dependence of the Lyapunov vectors upon the angle variable for $a \in [a_c, a_f)$ makes the torus-doubling bifurcation impossible, and in this case the smooth torus directly transforms into the SNA via a gradual fractalization (as described in Ref. [25]).

Now let us consider the process of destruction of smooth dependences $\mathbf{k}^{1,2}(\theta)$ in some detail. For this purpose we need to calculate the angle $\varphi(\theta)$ between leading and nonleading Lyapunov vectors $\mathbf{k}^{1,2}$ on the torus as a function of θ. Since we have chosen $|\mathbf{k}^{1,2}(\theta)|=1$, we immediately get

$$\varphi(\theta) = \arccos[\mathbf{k}^1(\theta) \cdot \mathbf{k}^2(\theta)].$$

Then we take the least of the two angles φ or $(\pi/2-\varphi)$. The plot of the function $\varphi(\theta)$ for $a=0.556$ (slightly below the critical value a_c) is shown in Fig. 3(a). This function is piecewise differentiable (several fractures on the plot are associated with our choice of $\varphi \in [0, \pi/2]$). One can see that the

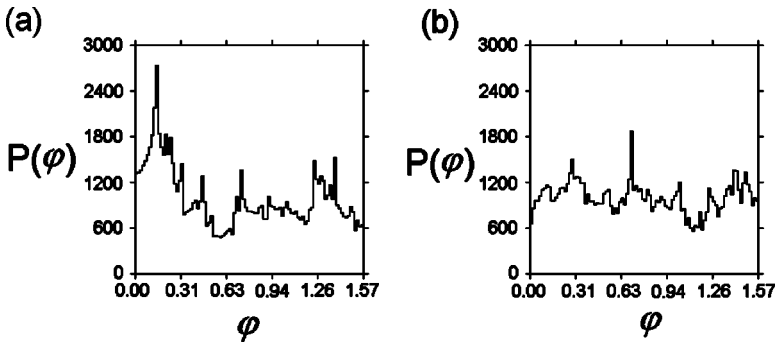

FIG. 4. Histograms of the angle φ between Lyapunov vectors: (a) for a trajectory on the torus at $a=0.6$, $\varepsilon=0.6$, (b) for a trajectory on SNA at $a=0.66$, $\varepsilon=0.6$. The length of trajectory segment is 10^5 iterations.

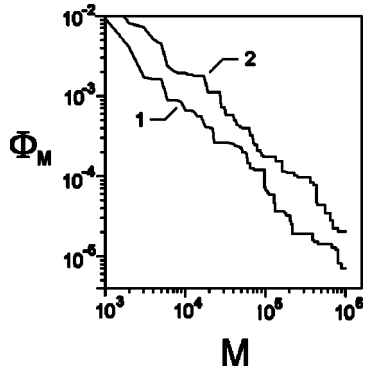

FIG. 5. Plot of the function Φ_M for 100 trajectories with randomly chosen initial angle variable on the torus (plot 1, $a=0.6$, $\varepsilon=0.6$) and on the SNA (plot 2, $a=0.66$, $\varepsilon=0.6$).

plot of $\varphi(\theta)$ approaches the axis $\varphi=0$ very closely. The minimum angle $\varphi_{\inf}=\min_{\theta\in[0,1)}\varphi(\theta)$ between the Lyapunov vectors decreases and becomes infinitely close to zero, as the parameter a approaches the critical value a_c; see Fig. 3(b). Actually it remains uncertain whether the minimum angle goes strictly to zero. However, in numerical experiments we failed to find a lower bound for the angle distinct from zero. Thus, we conjecture that the loss of smoothness of the dependences $\mathbf{k}^{1,2}(\theta)$ is associated with situations, when the leading and nonleading Lyapunov vectors $\mathbf{k}^1(\theta)$ and $\mathbf{k}^2(\theta)$ coincide at some values of the angle variable θ on the torus. Note that, due to ergodicity of the angle variable θ, coincidence of the vectors $\mathbf{k}^1$ and $\mathbf{k}^2$ at one point of the ergodic torus implies presence of a dense set of such coincidences in images and preimages of this point.

In order to confirm the conjecture made in the previous paragraph, let us consider the distributions of the angle φ along typical trajectories on invariant curve for values of a above the critical value a_c. Our interest is focused on the lower bound of such distributions. Since, in the numerical computations we deal with, the trajectory segments of a finite length, we will observe the minimum value of the angle φ obtained along sufficiently long segment of a typical trajectory. For a trajectory segment of M iterations starting from the initial phase θ_0 we define

$$\varphi_{\min}(\theta_0,M)=\min_{n=0,1,\ldots,M}\varphi(\theta_n).$$

Figure 4(a) shows a histogram of the distribution of the angle φ along a segment of a typical trajectory of length $M=10^5$ on the smooth torus at $a=0.6$. The histogram shows that the probability density function is nonzero for small angles φ. In Fig. 4(b) we see an analogous histogram of angles φ for a segment of trajectory on the SNA ($M=10^5$) at $a=0.66$. In both cases the angle $\varphi_{\min}(\theta_0,M)$ decreases and approaches arbitrarily close to zero as we examine longer and longer segments of the trajectory. This result does not depend upon our choice of the initial phase θ_0. To show it, let us consider the maximum value of $\varphi_{\min}(\theta_0,M)$ with respect to trajectories with different initial phases θ_0:

$$\Phi_M=\max_{\theta_0\in[0,1]}\varphi_{\min}(\theta_0,M).$$

A plot of this function obtained with an ensemble of 100 trajectories on a smooth torus (at $a=0.64$) with randomly chosen initial phases θ_0 is presented in the Fig. 5, plot 1. One can see that for sufficiently large M the function Φ_M behaves as

$$\Phi_M\sim M^{\gamma},$$

where $\gamma\simeq-1$. Thus, our conclusion concerning zero lower bound for the angle φ is valid for all or almost all trajectories on the smooth torus. Hence, we can neglect the dependence of the minimum angle $\varphi_{\min}$ upon the initial phase θ_0: $\varphi_{\min}=\varphi_{\min}(M)$. Note that the same results for the minimum angle $\varphi_{\min}$ were obtained for trajectories on SNA, as seen in plot 2 of Fig. 5, at $a=0.66$.

The same properties of the distribution of the angle φ were observed for trajectories on smooth torus and SNA at all tested values $a\in[a_c,a_f)$. In order to illustrate this statement, let us fix a length M of a trajectory segment and consider the dependence of the minimum angle $\varphi_{\min}$ upon the parameter a: $\varphi_{\min}=\varphi_{\min}(M,a)$. Figure 6 shows the dependences $\varphi_{\min}(a)$ for two fixed values $M=10^4$ (a) and $M=10^5$ (b). Comparison of these plots illustrates the effect of an increase in M. One can observe a significant (of an order of magnitude) decrease of the minimum angle $\varphi_{\min}$ as M grows from 10^4 to 10^5.

We also note the following fact as worthy of note. For the case of chaotic systems, interest immediately focuses on the properties of chaotic saddles (see Ref. [39] and works cited therein). The chaotic saddle is hyperbolic if all angles between the stable and unstable directions (which coincide with the Lyapunov vectors) are uniformly bounded away

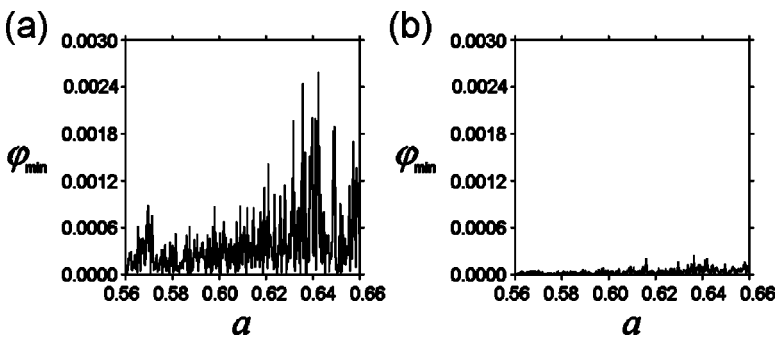

FIG. 6. The effect of increase of the trajectory segment length M on the minimum angle between Lyapunov vectors: dependence $\varphi_{\min}(M,a)$ versus a for (a) $M=10^4$ and (b) $M=10^5$.

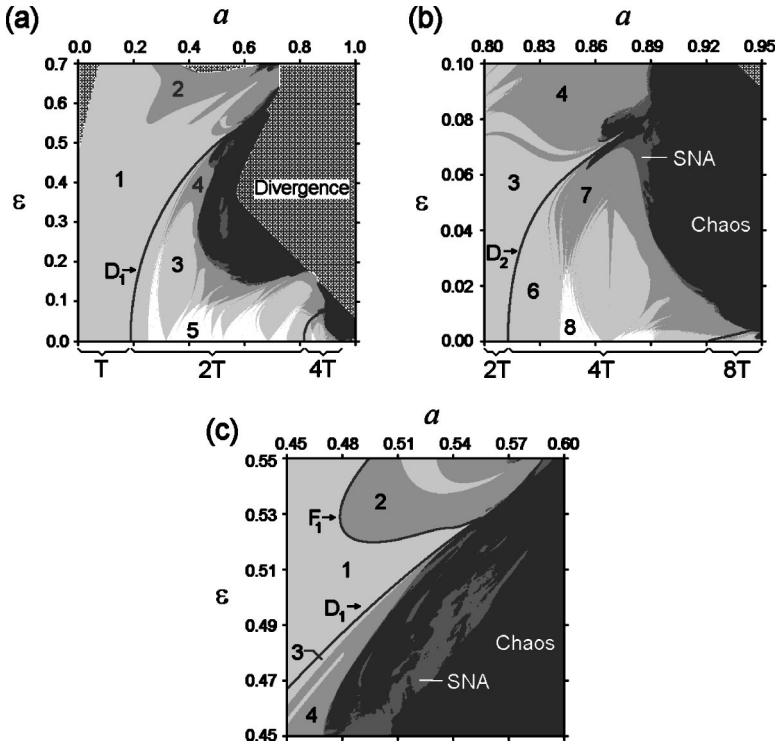

FIG. 7. Parts of the parameter plane of the map (2) at the fixed value $b=0.5$. The regions of existence of a torus T (**1**,**2**), double torus $2T$ (**3**,**4**,**5**), and quadruple torus $4T$ (**6**,**7**,**8**) are divided into subregions in accordance with smooth, nonsmooth, or undefined dependence of the Lyapunov vectors upon the angle variable. The light gray (**1**,**3**,**6**), gray (**2**,**4**,**7**), and white (**5**,**8**) tones denote the regions of smooth, nonsmooth, or undefined dependence, respectively. The regions of SNA and chaos are shown in dark gray and black, respectively. In the patterned areas the map (2) has no attractor. The curves D_1 and D_2 correspond to the first and second torus-doubling bifurcations. The curve F_1 between the regions **1** and **2** denotes the border of the loss of smoothness of the vector functions $\mathbf{k}^{1,2}(\theta)$. (a) The general parameter plane. (b) The enlarged fragment in the area of the second torus-doubling bifurcation. (c) The enlarged fragment near the terminal point of the first torus-doubling bifurcation curve.

from zero. Otherwise, the chaotic saddle is referred to as nonhyperbolic. The properties of the (non)hyperbolicity of chaotic saddles in the Hénon map were studied in Ref. [39]. In this context, our results for the distributions of angles between the Lyapunov vectors for trajectories on a smooth torus and a SNA seem rather intriguing. One can compare Figs. 4(a) and 4(b) of the current paper with the analogous Fig. 8(c) of Ref. [39] and our Figs. 6(a) and 6(b) with Figs. 11(a) and 11(b) of Ref. [39]. The numerical results for the angle distributions are very similar, although we consider nonchaotic trajectories on a smooth torus and a SNA, while the authors of the work [39] deal with nonhyperbolic chaotic saddles. Thus, we can conclude that on the route from quasiperiodicity to chaos the angles between the Lyapunov vectors may go to zero before the destruction of a regular motion and onset of a chaotic dynamics. We believe that this observation is interesting and may merit a special study.

IV. STRUCTURE OF THE PARAMETER SPACE OF THE QUASIPERIODICALLY FORCED HÉNON MAP

Let us now consider the configuration of regions of different dynamical behavior in the parameter space of the map (2). Figure 7 shows three fragments of the a-ε parameter plane at the fixed value $b=0.5$. In order to distinguish nonchaotic and chaotic dynamical regimes on the parameter plane, we calculate the largest nontrivial Lyapunov exponent σ_1. On the other hand, smooth tori and strange nonchaotic attractors may be distinguisehd via calculation of the phase sensitivity exponent δ, which measures the sensitivity of a trajectory on an attractor with respect to a variation of the angle variable θ (see Ref. [15]). Smooth attractors (e.g., torus T, double torus $2T$, quadruplicate torus $4T$, etc.) have a negative Lyapunov exponent ($\sigma_1<0$) without phase sensitivity ($\delta=0$). The symbols T, $2T$, and $4T$ below the planes indicate intervals of the parameter a, in which the respective smooth tori exist at $\varepsilon=0$. The light-gray tone corresponds to regions of quasiperiodic dynamics characterized by the smooth dependence of the Lyapunov vectors upon the angle variable on torus (the indices **1**, **3**, and **6** correspond to the tori T, $2T$, and $4T$, respectively). The gray tone shows the regions of tori with nonsmooth dependence of the Lyapunov vectors upon the angle variable (**2**, **4**, and **7** correspond to T, $2T$, and $4T$). In the regions shown in white the Lyapunov vectors on tori are not defined (**5** and **8** correspond to $2T$ and $4T$). The area of chaotic dynamics ($\sigma_1>0$) is shown in black. Between the regular and chaotic regimes, an SNA exists in the region shown in dark-gray tone. This intermediate type of attractor is characterized by negative Lyapunov exponent ($\sigma_1<0$) with high phase sensitivity ($\delta>0$). In the area filled by pattern, the map (2) has no attractor, and the trajectories escape to infinity.

Let us consider mechanisms of dynamical transitions in the parameter plane in some detail. In regions **1** and **2** the attractor of the system (2) is a smooth torus. In region **1** this torus is characterized by a smooth dependence of Lyapunov vectors $\mathbf{k}^{1,2}(\theta)$ upon the angle θ, as shown in Figs. 2(b) and 2(c). In region **2** the vector functions $\mathbf{k}^{1,2}(\theta)$ become nondifferentiable [see Figs. 2(d) and 2(e)]. The transition from **1** to **2** is associated with the mechanism described in the previous section.

When crossing the line D_1 on the border of the regions **1** and **3**, the torus T becomes unstable and bifurcates to the double torus $2T$. An example of the double torus of the map (2) at $a=0.315$, $\varepsilon=0.3$ (region **3**) is shown in Fig. 8(a). Since the double torus $2T$ consists of two smooth branches,

$$2T_1:\{(x,y,\theta) \in \mathbf{R}^2 \times \mathbf{T}^1 | x = x^{(1)}(\theta), y = y^{(1)}(\theta), \theta \in [0,1)\},$$

$$2T_2:\{(x,y,\theta) \in \mathbf{R}^2 \times \mathbf{T}^1 | x = x^{(2)}(\theta), y = y^{(2)}(\theta), \theta \in [0,1)\},$$

we need to introduce two pairs of vector functions $\mathbf{k}_i^{1,2}(\theta)$ $(i=1,2)$ to characterize the dependences of Lyapunov vectors upon the angle variable on the double torus. Let the pair of vector functions $\mathbf{k}_1^{1,2}(\theta)=(k_{x1}^{1,2}(\theta),k_{y1}^{1,2}(\theta),0)$ determine the leading and nonleading Lyapunov vectors on the branch T_1, while the pair $\mathbf{k}_2^{1,2}(\theta)=(k_{x2}^{1,2}(\theta),k_{y2}^{1,2}(\theta),0)$ be associated with the branch $2T_2$. In order to numerically obtain the value of the leading Lyapunov vector $\mathbf{k}_1^1(\theta_0)$ at the point $(x_0,y_0,\theta_0) \in 2T_1$, we can start iterating the map (6) from the initial angle θ_{-n} $[=\theta_0-n\omega \pmod 1]$, where n is a sufficiently large natural number, with an arbitrarily chosen initial vector $\mathbf{k}_{-n}$. Note that the variables x and y in the map (6) are functions of the angle variable θ, and in this case they must be defined as

$$x_j = \begin{cases} x^{(1)}(\theta_j), & j = 2m, \\ x^{(2)}(\theta_j), & j = 2m+1, \end{cases}$$

$$y_j = \begin{cases} y^{(1)}(\theta_j), & j = 2m, \\ y^{(2)}(\theta_j), & j = 2m+1, \end{cases} \tag{8}$$

where m is a natural number such that $0 \leqslant m \leqslant n/2$. Varying θ_0 within the interval $[0)$, we will obtain the full dependence $\mathbf{k}_1^1(\theta)$. On the other hand, in order to find the vector $\mathbf{k}_2^1(\theta_0)$ at the point $(x_0,y_0,\theta_0) \in 2T_2$, one should iterate the map (6) from the initial angle θ_{-n} with an arbitrarily chosen initial vector $\mathbf{k}_{-n}$ and with the following conditions for x and y:

$$x_j = \begin{cases} x^{(2)}(\theta_j), & j = 2m, \\ x^{(1)}(\theta_j), & j = 2m+1, \end{cases}$$

$$y_j = \begin{cases} y^{(2)}(\theta_j), & j = 2m, \\ y^{(1)}(\theta_j), & j = 2m+1. \end{cases} \tag{9}$$

In the same way, one can determine the nonleading Lyapunov vector $\mathbf{k}_1^2(\theta_0)$ or $\mathbf{k}_2^2(\theta_0)$. For this purpose one should iterate the map (7) from the initial angle θ_n $[=\theta_0 + n\omega \pmod 1]$, where n is a sufficiently large natural number, with an arbitrarily chosen initial vector $\mathbf{k}_n$, and the dependences $x=x(\theta)$ and $y=y(\theta)$ are given by formula (8) and (9).

The plots of the functions $\mathbf{k}_{x1}^1(\theta)$ and $\mathbf{k}_{x2}^1(\theta)$ at $a=0.315$ and $\varepsilon=0.3$ (region **3**) are presented in Fig. 8(b), while Fig. 8(c) shows the plots of $\mathbf{k}_{x1}^2(\theta)$ and $\mathbf{k}_{x2}^2(\theta)$. One can see that all these functions are smooth. Hence, the Lyapunov vectors smoothly depend upon the angle θ on the double torus at the respective parameter values. On the other hand, in region **4** the double torus is characterized by the nonsmooth dependence of Lyapunov vectors upon the angle variable. An example of the double torus of the map (2) at $a=0.33$ and $\varepsilon=0.3$ (region **4**) is presented in Fig. 8(d). Figures 8(e) and 8(f) show the plots of the nonsmooth functions $\mathbf{k}_{x1}^1(\theta)$ and $\mathbf{k}_{x1}^2(\theta)$ at the same parameter values. In region **5** a vicinity of the double torus is of a focal type: therefore, Lyapunov vectors are not defined. In this situation the attractors of the maps (6) and (7) represent three-frequency tori.

The line D_2 on the border of regions **3** and **6** [see the enlarged fragment of the parameter plane in the Fig. 7(b)] corresponds to the second doubling bifurcation, in which the double torus $2T$ bifurcates to the quadruplicate torus $4T$. The latter is characterized by four pairs of vector functions $\mathbf{k}_i^{1,2}(\theta)$ $(i=1,\ldots,4)$, which give the dependences of the Lyapunov vectors upon the angle variable θ on each of the four branches $4T_i$ $(i=1,\ldots,4)$ of the quadruplicate torus $4T$. The regions corresponding to smoothness and nonsmoothness of the vector functions $\mathbf{k}_i^{1,2}(\theta)$ $(i=1,\ldots,4)$ are denoted

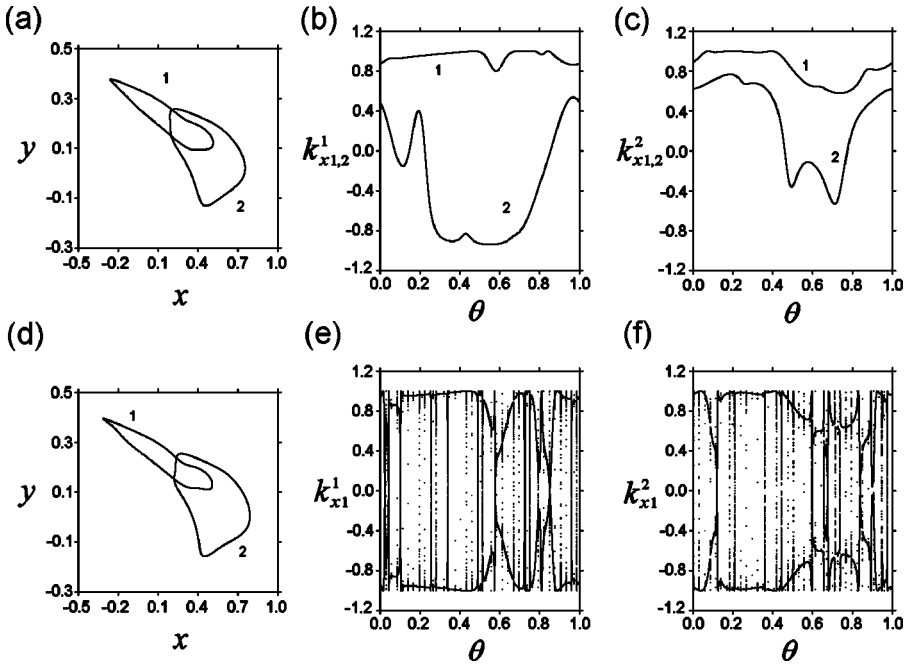

FIG. 8. (a) Attracting double torus of the map (2) at $a=0.315$, $\varepsilon=0.3$ (digits *1* and *2* are related to the branches $2T_1$ and $2T_2$). (b) The plots of the functions $k_{x1}^1(\theta)$ and $k_{x2}^1(\theta)$ at $a=0.315$, $\varepsilon=0.3$. (c) Plots of the functions $k_{x1}^2(\theta)$ and $k_{x2}^2(\theta)$ at $a=0.315$, $\varepsilon=0.3$. (d) Attracting double torus of the map (2) at $a=0.33$, $\varepsilon=0.3$. (e) Plot of the function $k_{x1}^1(\theta)$ at $a=0.33$, $\varepsilon=0.3$. (f) Plot of the function $k_{x1}^2(\theta)$ at $a=0.33$, $\varepsilon=0.3$.

as **6** and **7**, respectively. In region **8** the Lyapunov vectors are undefined. This corresponds to the focal structure of a vicinity of the quadruplicate torus $4T$.

Based on Fig. 7, one can make the following important observation: the torus-doubling bifurcations occurs on passage between the regions characterized by smooth dependence of the Lyapunov vectors on the torus upon the angle variable: $\mathbf{1}\to\mathbf{3}$, $\mathbf{3}\to\mathbf{6}$. Indeed, the smooth dependence of Lyapunov vectors upon the angle variable on the "parent" torus is necessary for the doubling bifurcation could take place, and the "newly born" torus is also characterized by smooth vector functions $k_i^{1,2}(\theta)$. Figure 7(c) shows the enlarged fragment of the parameter plane in the region where the termination of the torus-doubling line D_1 occurs. In order to understand the mechanism of this phenomenon, note that the line F_1 corresponding to the loss of smoothness of the vector functions $\mathbf{k}^{1,2}(\theta)$ intersects with the line D_1 at $(a_c^{(1)},\varepsilon_c^{(1)})\simeq(0.554\ 78, 0.528\ 46)$. If the parameter ε is fixed at $\varepsilon<\varepsilon_c^{(1)}$ and the parameter a is varied, one can observe a transition between the regions $\mathbf{1}\to\mathbf{3}$. For the case $\varepsilon>\varepsilon_c^{(1)}$ such transition becomes impossible due to the loss of smoothness of the vector-function $\mathbf{k}^{1,2}(\theta)$. Note that a vicinity of the torus-doubling terminal point contains parameter values related to the regions of different dynamical behavior: quasiperiodicity (**1**, **2**, **3**, **4**), SNA, and chaos.

The line of the second torus-doubling bifurcation D_2 terminates at $(a_c^{(2)},\varepsilon_c^{(2)})\simeq(0.873\ 64, 0.074\ 71)$. Although we did not study this phenomenon in detail, we found that it is also associated with the loss of the smoothness of the dependences of Lyapunov vectors upon the angle variable. For $\varepsilon<\varepsilon_c^{(2)}$ the double torus $2T$ may undergo bifurcation to the quadruple torus $4T$ under variation of the control parameter a. For $\varepsilon>\varepsilon_c^{(2)}$ such a bifurcation appears to be prevented by the loss of smoothness of the vector functions $\mathbf{k}_i^{1,2}(\theta)$ $(i=1,2)$.

On the other hand, one can see that the transitions from quasiperiodicity to SNA occur on coming out of the regions of quasiperiodic regimes characterized by nonsmooth vector functions $\mathbf{k}_i^{1,2}(\theta)$: $\mathbf{2}\to$SNA, $\mathbf{4}\to$SNA, and $\mathbf{7}\to$SNA. Note that a specific mechanism of the birth of an SNA depends upon the choice of the parameter values. For the case of the transition $\mathbf{2}\to$SNA, this mechanism may consist in a gradual fractalization of the torus [25,30] or an intermittency [32,33]. For the the case of the transitions $\mathbf{4}(\mathbf{7})\to$SNA, a collision of the attracting double (quadruple) torus with a parent saddle torus (Heagy and Hammel mechanism [24,30]) may occur besides torus fractalization and intermittency. All of these mechanisms have irregular, phase-dependent character.

Thus, the appearance of a nonsmooth dependence of the Lyapunov vectors upon the angle variable on the torus always precedes the destruction of a regular quasiperiodic motion and the onset of a strange nonchaotic attractor via phase-dependent mechanisms. On the contrary, regular torus-doubling bifurcations require the existence of a smooth vector-functions $\mathbf{k}_i^{1,2}(\theta)$. In this sense we can claim that calculations of the Lyapunov vectors make it possible to predict regularity or irregularity of further torus bifurcations.

V. ANALYSIS OF RATIONAL APPROXIMATIONS

Another way to explain the mechanism of termination of the torus-doubling bifurcation line is provided by the method of rational approximation, which is widely used for analysis of Hamiltonian and dissipative systems. In application to the quasiperiodically forced systems the idea of the method consists in the following (see Refs. [5–7,15]). The irrational parameter of frequency ω in the map (2) can be approximated by a sequence rational values ω_k, such that $\omega=\lim_{k\to\infty}\omega_k$. For the case of the golden mean, the sequence of approximants $\{\omega_k\}_{k=0,1,\ldots,\infty}$ is given by the ratios of Fibonacci numbers: $\omega_k=F_{k-1}/F_k$, where $F_{k+1}=F_k+F_{k-1}$ with $F_0=0$ and $F_1=1$. For a definite level of approximation k, we consider an ensemble of maps

$$x_{n+1}=a-x_n^2+y_n+\varepsilon\cos 2\pi\theta_n,$$

$$y_{n+1}=bx_n,$$

$$\theta_{n+1}=\theta_n+\omega_k\ (\mathrm{mod}\ 1), \tag{10}$$

which are forced periodically with the same rational frequency ω_k and with different values of the initial angle θ_0. The attractor of the map (10) depends upon the initial angle θ_0. Changing θ_0 continuously in the whole interval $[0,1/F_k]$, we obtain the kth approximation of the attractor of the map (2) as a union of all occurring attractors of the map (10). We suppose that the properties of the original system (2) can be obtained in the quasiperiodic limit at $k\to\infty$.

An approximating set of order k for an attracting torus represents a smooth set of stable periodic orbits of period F_k. Note that the approximating orbits may be of two types: node and focus. Let us consider a periodic orbit of the map (10) that starts from the initial angle θ_0: $(x_0,y_0,\theta_0),(x_1,y_1,\theta_1),\ldots,(x_{F_k-1},y_{F_k-1},\theta_{F_k-1})$. The monodromy matrix of the periodic orbit is

$$\hat{\mathbf{J}}^{(F_k)}(x_0,y_0,\theta_0)=\hat{\mathbf{J}}(x_{F_k-1},y_{F_k-1},\theta_{F_k-1})\times\hat{\mathbf{J}}(x_{F_k-2},y_{F_k-2},\theta_{F_k-2})\cdots\hat{\mathbf{J}}(x_0,y_0,\theta_0). \tag{11}$$

Since the given orbit belongs to a smooth approximating set, the variables x and y in Eq. (11) are functions of the angle variable θ [$x_0=x(\theta_0)$, $y_0=y(\theta_0)$, etc.], and we can write simply $\hat{\mathbf{J}}^{(F_k)}(\theta_0)$. The type of the periodic orbit is determined by the values of the multipliers $\mu_{1,2}^{F_k}$, which represent the nontrivial eigenvalues of the matrix $\hat{\mathbf{J}}^{(F_k)}(\theta_0)$. The multipliers depend upon the initial angle of the orbit θ_0: $\mu_{1,2}^{F_k}=\mu_{1,2}^{F_k}(\theta_0)$. If the multipliers are real, the orbit is of a nodal type; otherwise, it is a focus. The Lyapunov exponents of the orbit are defined as

$$\sigma_{1,2}^{F_k}(\theta_0)=(1/F_k)\ln|\mu_{1,2}^{F_k}(\theta_0)|.$$

Note that the values of $\sigma_{1,2}^{F_k}$ may be interpreted as approximants of local (finite-time) Lyapunov exponents over F_k iterations of the quasiperiodically forced Hénon map.

In the same way, approximants of the leading and nonleading Lyapunov vectors $\mathbf{k}_{F_k}^{1,2}(\theta_0)$ can be defined as eigenvectors of the matrix $\hat{\mathbf{J}}^{(F_k)}(\theta_0)$,

$$\hat{\mathbf{J}}^{(F_k)}(\theta_0)\mathbf{k}_{F_k}^{1,2}(\theta_0) = \mu_{1,2}^{F_k}(\theta_0)\mathbf{k}_{F_k}^{1,2}(\theta_0),$$

and they depend upon the initial angle θ_0. Let us analyze the structure of the approximating set of periodic orbits, corresponding to different values of the initial angle θ_0. In the quasiperiodic limit ($k\to\infty$) we find the following three cases to be possible.

(C1) As the value of θ_0 is varied, one can observe a transition of the multipliers $\mu_{1,2}^{F_k}(\theta_0)$ from real to complex-conjugate values. Thus, the approximating set includes periodic orbits of two types: nodal and focal. Such "mixed" structure of the approximating set of orbits persists as the order of approximation k is increased.

(C2) The multipliers $\mu_{1,2}^{F_k}(\theta_0)$ are real for all θ_0 from the interval $[0,1/F_k)$. Thus, the approximating set consists of periodic orbits of nodal type. However, for some values of θ_0 the condition $|\mu_1^{F_k}| \geqslant |\mu_2^{F_k}|$ holds, while for other values of θ_0 the opposite is valid: $|\mu_2^{F_k}| > |\mu_1^{F_k}|$. In other words, this set has nonhomogeneous structure in the sense that the leading Lyapunov vector may transform into the nonleading one and back, as the value of θ_0 is varied. Such "nonuniform" structure of the approximating set of orbits persists as the order k of the approximation is increased.

(C3) The approximating set for the smooth torus consists of periodic orbits of the same type (nodal). The set has uniform structure in the sense of absence of the exchange of the leading and nonleading Lyapunov vectors.

In cases (C1) and (C2) the structure of the approximating set can be referred to as "phase dependent." In the quasiperiodic limit, the phase-dependent approximating set forms a torus which is characterized by a nonsmooth dependence of the Lyapunov vectors $\mathbf{k}^{1,2}(\theta)$ upon the angle variable θ. On the other hand, case (C3) corresponds to a situation when the dependencies $\mathbf{k}^{1,2}(\theta)$ are smooth.

Before a study of the structure of approximating set, note that the one-time-iterated map (10) has negative Jacobi determinant ($J=-b$). The superposition of F_k maps (10) will possess the Jacobian $J=(-b)^{F_k}$. Hence, we need to consider separately rational approximants $\omega_k = F_{k-1}/F_k$ with odd and even periods F_k. Indeed, the matrix $\hat{\mathbf{J}}^{(F_k)}(\theta_0)$ has the form

$$\hat{\mathbf{J}}^{(F_k)}(\theta_0) = \begin{bmatrix} J_{11}(\theta_0) & J_{12}(\theta_0) & J_{13}(\theta_0) \\ J_{21}(\theta_0) & J_{22}(\theta_0) & J_{23}(\theta_0) \\ 0 & 0 & 1 \end{bmatrix}.$$

The nontrivial multipliers of the periodic orbit $\mu_{1,2}^{F_k}(\theta_0)$ are defined as

$$\mu_{1,2}^{F_k}(\theta_0) = S(\theta_0)/2 \pm \sqrt{[S(\theta_0)/2]^2 - (-b)^{F_k}},$$

where $S(\theta_0) = J_{11}(\theta_0) + J_{22}(\theta_0)$. Since we have originally chosen $b>0$, the multipliers are always real for the case of odd values of F_k. Hence, all the approximating orbits of odd period are nodal. On the other hand, for even F_k, values of the angle θ_0 can exist such that the condition

$$(S(\theta_0)/2)^2 < b^{F_k} \tag{12}$$

holds. For this case, the approximating set can possess orbits of both nodal and focal type.

As an example, let us consider the system (2) at the parameter values $a=0.34$, $\varepsilon=0.6$, and $b=0.5$, which correspond to the case of existence of the nonsmooth dependences $\mathbf{k}^{1,2}(\theta)$. In order to illustrate the existence of phase-dependent structure of the approximating set of periodic orbits, we have computed the nontrivial Lyapunov exponents $\sigma_{1,2}^{F_k} = (1/F_k)\ln|\mu_{1,2}^{F_k}|$ as functions of the initial angle variable θ_0 within the interval $[0,1/F_k)$. Figure 9(a) shows plots of the functions $\sigma_{1,2}^{F_k}(\theta_0)$ for the odd period of approximation: $F_k=55$. The exponent $\sigma_1^{F_k}$ corresponds to the negative multiplier ($\mu_1^{F_k}<0$), while the exponent $\sigma_2^{F_k}$ ($=\ln|b|-\sigma_1^{F_k}$) corresponds to the positive multiplier ($\mu_2^{F_k}>0$). One can see that the interval $[0,1/F_k)$ turns out to be subdivided into three segments: **A**, **B**, and **C**. Within the subintervals **A** and **C** the condition $-\infty<\sigma_2^{F_k}<(1/2)\ln|b|<\sigma_1^{F_k}<0$ holds (respectively, $0<\mu_2^{F_k}<b^{F_k/2}<-\mu_1^{F_k}<1$). Thus, the approximating Lyapunov vector $\mathbf{k}_{F_k}^1$ is leading within these subintervals, and the exponent $\sigma_1^{F_k}$ is the largest of finite-time Lyapunov exponents. In the subinterval **B** the backward condition $-\infty<\sigma_1^{F_k}<(1/2)\ln|b|<\sigma_2^{F_k}<0$ holds (respectively, $0<\mu_1^{F_k}<b^{F_k/2}<-\mu_2^{F_k}<1$). Hence, the approximating Lyapunov vector $\mathbf{k}_{F_k}^2$ appears to be leading in the subinterval **B**, and the exponent $\sigma_2^{F_k}$ becomes the largest.[4] On the border of the intervals there are two of such points $\theta_{1,2}^*$, where $\mu_2^{F_k}(\theta_{1,2}^*) = -\mu_1^{F_k}(\theta_{1,2}^*) = b^{F_k/2}$. We have tested rational approximants with large odd periods F_k up to $F_k=4181$ and found that the structure of the interval $[0,1/F_k)$ remains qualitatively the same as the level k of rational approximant increases. However, the quantitative features of the interval structure may change with k. Let us denote the relative lengths of the subintervals **A**, **B**, and **C** as p_A, p_B, and p_C, respectively (note that the sum length of all subintervals is normalized to unity: $p_A+p_B+p_C=1$). Figure 9(b) shows the dependence of the relative length p_{A+C} ($=p_A+p_C$) upon k. One can see that the dependence has irregular character. Note that none of the two components (p_{A+C} and p_B) decays to zero as the level k increases.

Figure 9(c) shows the dependences of the Lyapunov exponents $\sigma_{1,2}^{F_k}$ upon the initial angle θ_0 for the approximating set of periodic orbits in the case of even period $F_k=34$. In this figure the interval $[0,1/F_k)$ is divided into five subintervals. Within the subintervals **A**, **C**, and **E** the values of multipliers $\mu_{1,2}^{F_k}$ are real. Hence, the corresponding stable periodic orbits are of nodal type. On the other hand, within subintervals **B** and **D** the condition (12) holds. The periodic orbits within subintervals **B** and **D** are characterized by

[4]Note that the values of $\sigma_{1,2}^{F_k}$ are negative over all the intervals **A**, **B**, and **C**, and the approximating set consists of stable periodic orbits only. Since $\sigma_{1,2}^{F_k}$ may be interpreted as approximants of finite-time (over F_k iterations) Lyapunov exponents, we see that the appearance of a nonsmooth dependence of the Lyapunov vectors upon the angle variable does not result in the appearance of a local instability.

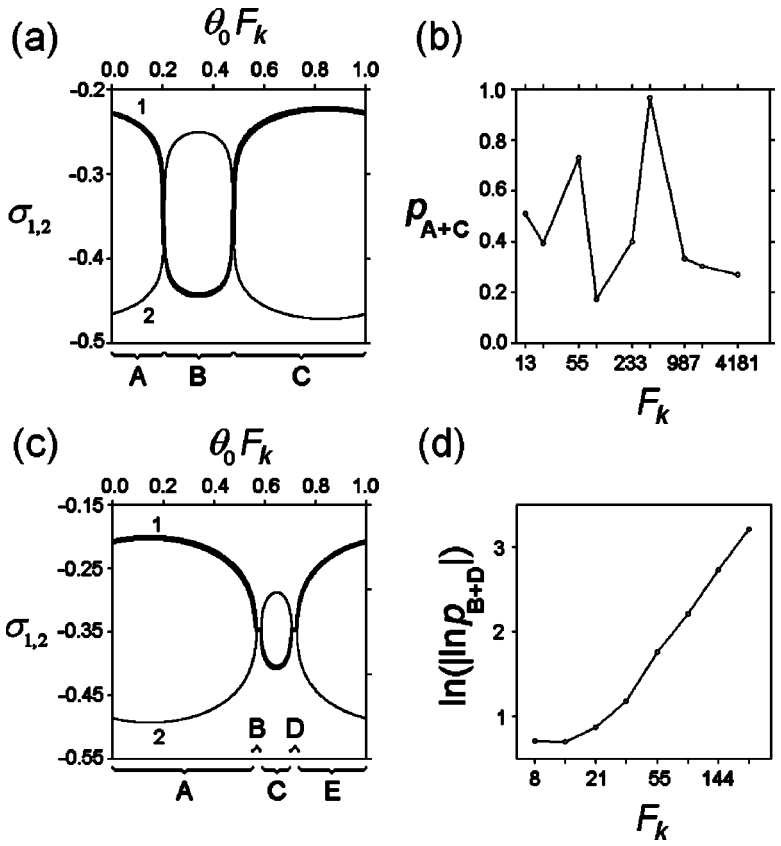

FIG. 9. (a) Plots of the functions $\sigma_1(\theta_0)$ (thick curve) and $\sigma_2(\theta_0)$ (thin curve) for $F_k=55$ at $a=0.34$, $\varepsilon=0.6$. (b) Dependence of the sum length p_{A+C} upon the period F_k (logarithmic scale) of approximation. (c) Plots of the functions $\sigma_1(\theta_0)$ (thick curve) and $\sigma_2(\theta_0)$ (thin curve) for $F_k=34$ at $a=0.34$, $\varepsilon=0.6$. (d) Dependence of the sum length p_{B+D} (double logarithmic scale) upon the period F_k (logarithmic scale) of approximation.

complex-conjugate multipliers $[\mu_1^{F_k}=(\mu_2^{F_k})^*]$. The transition from region **A** to region **B** implies a change of the nodal type of orbit to the focal type. Analyzing the structure of the interval $[0,1/F_k)$ under increase of k, we found that it remains qualitatively the same for large, even F_k. However, the quantitative features change with k. The sum length of the intervals of nodal orbits $p_{\mathbf{A+C+E}}$ $(=p_{\mathbf{A}}+p_{\mathbf{C}}+p_{\mathbf{E}})$ dominates over the sum length of the intervals of focal orbits $p_{\mathbf{B+D}}$ $(=p_{\mathbf{B}}+p_{\mathbf{D}})$. In Fig. 9(d) we have plotted the sum length $p_{\mathbf{B+D}}$ (double-logarithmic scale) versus the period F_k (logarithmic scale). Since the condition (12) is applicable to both even and odd approximations, we consider both even and odd periods F_k in order to obtain a representative plot. One can see that the points on the plot can be fitted by a straight line for sufficiently large F_k. Hence, the relative length p_{B+D} decays as exponent of the period F_k of approximation.[5]

If the approximating sets of some torus possess phase-dependent nonuniformity of the described type and this nonuniformity persists in the quasiperiodic limit, the corresponding torus cannot undergo a doubling bifurcation. Indeed, let us consider the mechanism of the doubling bifurcation of a torus from the viewpoint of bifurcations of the approximating periodic orbits. For the case of an approximation with odd period F_k, each periodic orbit of the set undergoes doubling bifurcation along the leading Lyapunov direction, which is associated with the negative multiplier μ_2. However, the Lyapunov vector $\mathbf{k}^1$ appears to be leading only within segments **A** and **C** of the interval $[0,1/F_k)$, as we have shown above. Within the segment **B** the condition holds $-b^{F_k/2}<\mu_2^{F_k}<0$. Hence, the periodic orbits within the segment **B** cannot undergo a doubling bifurcation. For the case of an approximation with even period F_k, there are two subintervals (**B** and **D**), in which the periodic orbits are characterized by complex-conjugate multipliers. Obviously, the respective periodic orbits cannot undergo doubling bifurcation.

Note that the phase-dependent nonuniformity in the structure of the approximating set makes other regular torus bifurcations (symmetry breaking, saddle-node) impossible, besides the torus-doubling bifurcation. Indeed, regular torus bifurcation occurs when all orbits corresponding to different initial angles θ_0 on a torus bifurcate in a similar way. The last requirement is obviously impossible for the case of the phase-dependent nonuniform structure of the approximating set described above. Hence, the given torus can undergo evolution and destruction according to phase-dependent mechanisms only. In other words, under a variation of the parameters of the map (2) such a torus disappears with the onset of a strange nonchaotic attractor or of the divergence of trajectories. This conclusion is confirmed by the numerical observations made in Sec. IV on the structure of the parameter space of the quasiperiodically forced Hénon map.

VI. CONCLUSION

In the present paper we have observed a transition which consists of the appearance of a nonsmooth dependence of the

[5]This result correlates with an analogous exponent law obtained for the rational approximations of the phase-dependent saddle-node bifurcation in the quasiperiodically forced circle map (Ref. [41]). We suppose this coincidence to be not fortuitous and to indicate a close relationship between the maps in Lyapunov space (6) and (7) and the quasiperiodically forced circle maps. This problem merits a special study.

Lyapunov vectors upon the angle variable on torus in the quasiperiodically forced Hénon map. Although the attractor of the system typically remains a smooth torus after such transition, this torus cannot undergo regular doubling bifurcations. We have shown that this transition terminates the line of torus-doubling bifurcation on the parameter plane of the model map and restricts the number of torus-doubling bifurcations on the route to chaos. The presence of a smooth or nonsmooth dependence of the Lyapunov vectors upon the angle variable on the torus determines whether torus bifurcations under variation of the parameters of the system will be regular or irregular. The transition always precedes the destruction of quasiperiodic motion and the birth of a strange nonchaotic attractor via irregular (phase-dependent) mechanisms.

We believe that the arguments of this paper concerning the mechanism of torus-doubling bifurcation can also be applied to other regular torus bifurcations—namely, symmetry breaking, transcritical, and saddle-node bifurcations. One can show that the existence of a smooth dependence of the Lyapunov vectors upon the angle variable on a torus is a necessary condition for the possibility of these regular torus bifurcations. Therefore, we suppose that the new phenomenon, which consists in the appearance of a nonsmooth dependence of the Lyapunov vectors upon the angle variable on the torus, plays a key role in different scenarios for the transition from regular motion to chaos in quasiperiodically forced systems.

Of course, in a real physical system some noise is inevitable. The question arises whether calculations of the Lyapunov vectors are reliable in real systems. To answer it, one can consider maps in the Lyapunov space (6) and (7) with an additional condition $x_n = x(\theta_n) + \gamma\xi_n$, where ξ_n is a noise variable and γ is a noise amplitude parameter. According to the results of [40], an SNA in a quasiperiodically forced systems is robust with respect to addition of a small noise signal. Hence, the dynamical regimes in the Lyapunov maps would not change due to a small noise. Therefore, we expect our analysis to be valid in real oscillatory systems under external quasiperiodic forcing in the presence of noise.

ACKNOWLEDGMENTS

The work was supported by the Russian Foundation of Basic Research (Grant No. 03-02-16074), CRDF (BRHE REC-006 ANNEX BF4M06, Y2-P-06-16), and by the grant of the UK Royal Society. The authors thank S.P. Kuznetsov for useful discussions.

[1] L. D. Landau, C. R. (Dokl.) Acad. Sci. URSS **44**, 311 (1944).
[2] D. Ruelle and F. Takens, Commun. Math. Phys. **20**, 167 (1971).
[3] S. Newhouse, D. Ruelle, and F. Takens, Commun. Math. Phys. **64**, 35 (1979).
[4] L. P. Shilnikov, in *Nonlinear and Turbulent Processes* (Gordon and Breach, Chur, Switzerland, 1984), Vol. 2.
[5] M. J. Feigenbaum, L. P. Kadanoff, and S. J. Shenker, Physica D **5**, 370 (1982).
[6] D. Rand, S. Ostlund, J. Sethna, and E. D. Siggia, Phys. Rev. Lett. **49**, 132 (1982).
[7] S. Ostlund, D. Rand, J. Sethna, and E. Siggia, Physica D **8**, 303 (1983).
[8] V. S. Anishchenko, T. E. Letchford, and M. A. Safonova, Izv. Vyssh. Uchebn. Zaved., Radiofiz. **27**, 565 (1984).
[9] K. Kaneko, Prog. Theor. Phys. **69**, 1806 (1983).
[10] J. Stavans, F. Heslot, and A. Libchaber, Phys. Rev. Lett. **55**, 596 (1985).
[11] E. G. Gwinn and R. M. Westervelt, Phys. Rev. Lett. **59**, 157 (1987).
[12] I. S. Aranson and N. F. Rulkov, J. Tech. Phys. **58**, 1656 (1988).
[13] T. Yazaki, Phys. Rev. E **48**, 1806 (1993).
[14] C. Grebogi, E. Ott, S. Pelikan, and J. A. Yorke, Physica D **13**, 261 (1984).
[15] A. Pikovsky and U. Feudel, Chaos **5**, 253 (1995).
[16] S. P. Kuznetsov, A. S. Pikovsky, and U. Feudel, Phys. Rev. E **51**, R1629 (1995).
[17] M. Ding, C. Grebogi, and E. Ott, Phys. Lett. A **137**, 167 (1989).
[18] B. R. Hunt and E. Ott, Phys. Rev. Lett. **87**, 254101 (2001).
[19] J. Stark, Physica D **109**, 163 (1997).
[20] G. Keller, Fundam. Math. **151**, 139 (1996).
[21] A. Pikovsky and U. Feudel, J. Phys. A **27**, 5209 (1994).
[22] U. Feudel, A. Pikovsky, and A. Politi, J. Phys. A **29**, 5297 (1996).
[23] S. P. Kuznetsov, Pis'ma Zh. Eksp. Teor. Fiz. **39**, 113 (1984) [JETP Lett. **39**, 113 (1984)].
[24] J. F. Heagy and S. M. Hammel, Physica D **70**, 140 (1994).
[25] T. Nishikawa and K. Kaneko, Phys. Rev. E **54**, 6114 (1996).
[26] S. Kuznetsov, U. Feudel, and A. Pikovsky, Phys. Rev. E **57**, 1585 (1998).
[27] A. Prasad, V. Mehra, and R. Ramaswamy, Phys. Rev. E **57**, 1576 (1998).
[28] A. Venkatesan and M. Lakshmanan, Phys. Rev. E **63**, 026219 (2001).
[29] A. Witt, U. Feudel, and A. Pikovsky, Physica D **109**, 180 (1997).
[30] O. Sosnovtseva, U. Feudel, J. Kurths, and A. Pikovsky, Phys. Lett. A **218**, 255 (1996).
[31] H. M. Osinga and U. Feudel, Physica D **141**, 54 (2000).
[32] A. Prasad, V. Mehra, and R. Ramaswamy, Phys. Rev. Lett. **79**, 4127 (1997).
[33] S.-Y. Kim, W. Lim, and E. Ott, Phys. Rev. E **67**, 056203 (2003).
[34] B. P. Bezruchko, S. P. Kuznetsov, and Y. P. Seleznev, Phys. Rev. E **62**, 7828 (2000).
[35] T. Zhou, F. Moss, and A. Bulsara, Phys. Rev. A **45**, 5394 (1992).
[36] A. Jalnine (unpublished).
[37] S.-Y. Kim (unpublished).
[38] A. Katok and B. Hasselblatt, *Introduction to the Modern*

Theory of Dynamical Systems (Cambridge University Press, Cambridge, England, 1995).

[39] Y.-C. Lai, C. Grebogi, J. A. Yorke, and I. Kan, Nonlinearity **6**, 779 (1993).

[40] I. A. Khovanov, N. A. Khovanova, P. V. E. McClintock, and V. S. Anishchenko, Phys. Lett. A **268**, 315 (2000).

[41] U. Feudel, A. S. Pikovsky, and J. Kurths, Physica D **88**, 176 (1995).